View metadata, citation and similar papers at core.ac.uk

brought to you by CORE

provided by Elsevier - Publisher Connector

Journal of Electroanalytical Chemistry 734 (2014) 43–52

Contents lists available at ScienceDirect

Journal of Electroanalytical Chemistry

journal homepage: www.elsevier.com/locate/jelechem

Combined photoelectrocatalytic/electro-Fenton process using a Pt/TiO_2NTs photoanode for enhanced degradation of an azo dye: A mechanistic study

Lucio C. Almeida *, Bianca F. Silva, Maria V.B. Zanoni

Institute of Chemistry of Araraquara, Department of Analytical Chemistry, UNESP, Rua Francisco Degni, 55, 14800-900 Araraquara, SP, Brazil

ARTICLE INFO

Article history:
Received 15 June 2014
Received in revised form 23 September 2014
Accepted 29 September 2014
Available online 20 October 2014

Keywords:
Electro-Fenton
Photoelectrocatalysis
Acid Red 29
Oxidation products
Pt decorated TiO_2NTs photoanode
Wastewater treatment

ABSTRACT

The combined photoelectrocatalytic/electro-Fenton (PEC/EF) process containing a Pt/TiO_2NTs photoanode and an air-diffusion PTFE cathode is investigated in the degradation of the Acid Red 29 (AR29) dye. The photoelectrocatalytic (PEC), electro-Fenton (EF) and photoelectrocatalytic/electro-Fenton (PEC/EF) processes are compared in the performance of dye treatment. The mineralisation ability of the AR29 dye increased in the sequence PEC < EF < PEC/EF with total organic carbon (TOC) decays of 81%, 90% and 98%, respectively. The AR29 decays followed a pseudo first-order kinetic. The higher mineralisation capacity obtained for the PEC/EF process in comparison with the PEC and EF processes was ascribed to the additional production of ·OH by the photolytic reactions in bulk and on the Pt/TiO_2NTs surface. The synergetic effect from the photocatalytic reduction of H_2O_2 onto the electrode surface (which minimises the electron/hole pair recombination) and the photolysis of Fe(III)–carboxylate complexes also enhanced the degradation efficiency of the coupled process. Finally, a plausible pathway for AR29 degradation via the PEC/EF process was proposed based on the by-products detected by HPLC and LC–MS/MS.

© 2014 Elsevier B.V. All rights reserved.

1. Introduction

A large variety of electrochemical advanced oxidative processes (EAOPs), such as photoelectrocatalysis (PEC) [1–4], anodic oxidation (AO) [5], electro-Fenton (EF) [6,7] and photoelectro-Fenton (PEF) [8–10], have been employed in the oxidation and/or removal of organic contaminants. These methodologies are based on the generation of the strong hydroxyl radical (·OH), which confers a high oxidation power for the degradation of persistent organic pollutants (POPs) [11].

Among a large variety of EAOPs, electrochemical techniques based on Fenton's reaction such as electro-Fenton (EF) and photo-electro-Fenton (PEF) processes have been widely employed in the degradation of herbicides [11–13], pharmaceuticals [10,14] and textile dyes [6,8,9,15]. These processes consist of the continuous and efficient production of H_2O_2 in acid medium via the two-electron reduction of O_2 gas at carbonaceous cathodes, such as carbon-PTFE gas diffusion electrodes [6,9–11], graphite-felt [16], activated carbon fibre [17] and BBD electrodes [13], by the following reaction (1):

$$O_2 + 2H^+ + 2e^- \rightarrow H_2O_2 \quad (1)$$

The addition of small amounts of Fe^{2+} ion to the solution reacts with the electrogenerated H_2O_2 in the acid medium to form homogeneous Fe^{3+} and ·OH from the classical Fenton's reaction (2) [18]:

$$Fe^{2+} + H_2O_2 + H^+ \rightarrow Fe^{3+} + {}^{\cdot}OH + H_2O \quad (2)$$

The catalytic reaction (2) is propagated by the cathodic reduction of Fe^{3+} ions at the cathode surface to regenerate Fe^{2+} ions (reaction (3)), allowing the dehydrogenation and hydroxylation of organic contaminants via non-selective attack of ·OH, leading to total mineralisation [18,19].

$$Fe^{3+} + e^- \rightarrow Fe^{2+} \quad (3)$$

Electrolysed dye solutions under EF conditions may also be exposed to UV irradiation by an artificial source, termed the photo-electro-Fenton (PEF) process [8,11,13], which is the basis for improving the reaction as a treatment method for organic contaminants. In this process, the UV irradiation can also accelerate the mineralisation of organic contaminants by the photolysis of Fe(III) complexes with carboxylic acids formed during the process, as shown in reaction (4). Therefore, there is an enhancement of Fe^{2+}

* Corresponding author. Tel.: +55 16 3301 9740.
E-mail address: luciobonn@gmail.com (L.C. Almeida).

http://dx.doi.org/10.1016/j.jelechem.2014.09.035
1572-6657/© 2014 Elsevier B.V. All rights reserved.

regeneration and additional ·OH production by the photochemical reduction of $Fe(OH)^{2+}$ complexes according to reaction (5) [9,20,21]:

$$Fe(OOCR)^{2+} + h\nu \rightarrow Fe^{2+} + CO_2 + R^{\cdot} \quad (4)$$

$$Fe(OH)^{2+} + h\nu \rightarrow Fe^{2+} + {}^{\cdot}OH \quad (5)$$

Additionally, the direct photolysis of hydrogen peroxide (reaction (6)) may favour an additional formation of ·OH, even in smaller proportions compared with reactions (2) and (5) [22].

$$H_2O_2 + h\nu \rightarrow {}^{\cdot}OH + {}^{\cdot}OH \quad (6)$$

To achieve a better performance in the EF and PEF processes, the couplings of different electrochemical and/or photochemical methodologies have been investigated. In this way, Khataee et al. studied PEF coupling by using a carbon coated graphite plate nanotube as a cathode and TiO_2 nanoparticles (Degussa P25) immobilised on glass plates for the treatment of a mixture of dyes [23]. Zarei et al. employed a combined PEF/photocatalytic (PEF/PC) process with a carbon nanotube–polytetrafluoroethylene (CNT–PTFE) electrode for the treatment of the basic red 46 azo dye [24]. Recently, the degradation of Rhodamine B was investigated by Ding et al., employing a new system by coupling photo-electrochemical/electro-Fenton processes in an undivided cell and applying a Bi_2WO_6/FTO glass plate as a photoanode [25]. Based on these works, the coupling of photocatalytic/electro-Fenton (PC/EF) processes in an undivided cell indicated that there is significant enhancement in the efficiency of the EF process, motivating new studies on the subject.

The use of photoelectrocatalytic processes by using semiconductor materials such as TiO_2 has been explored to treat several organic pollutants [26]. Among them, the modification/incorporation of metal nanoparticles, such as Pt [2,27,28], Au [29] and Ag [30], into the lattice of this semiconductor material has attracted attention. The decoration of semiconductor materials with metal nanoparticles has focused on decreasing band gap values, which limits their photoactivities at low wavelengths [31]. Furthermore, the metal insertion on semiconductor surfaces can reduce electron–hole recombination because the Fermi levels of these metal are lower than the TiO_2 conduction band when deposited onto the semiconductor surface [32,33]. Therefore, the introduction of metal nanoparticles onto the TiO_2 surface can enhance its oxidation capacity of organic contaminants when applied as the photoanode in photoelectrocatalytic processes [2,27,31]. Previously, we have reported the preparation, characterisation and application of TiO_2 nanotube arrays decorated with Pt nanoparticles (Pt/TiO_2-NTs) as photoelectrodes in the degradation/mineralisation of Acid Red 29 (AR29) [2]. This photoelectrode exhibits an intense absorption peak in the visible region, significantly decreasing its band gap energy and increasing the degradation efficiency. However, the process presents good efficiency only for diluted solutions.

In context, the aim of this work was to investigate the mineralisation of azo dye solutions by using a coupling photoelectrocatalytic/electro-Fenton (PEC/EF) process containing a Pt/TiO_2NTs photoanode and an air-diffusion PTFE cathode. The textile Acid Red 29 dye (AR29) was chosen as a model compound to compare the degradation efficiency of the coupling PEC/EF process with the EF and PEC processes (dye structure in Table 1). This azo dye was used because approximately 70% of the dyes consumed in the world belong to the class of azo dyes [34], which can pose certain environmental risks due to their carcinogenic and mutagenic properties [35,36]. The performance of the PEC/EF system was evaluated by comparison with the conventional PEC and EF processes by monitoring the decolourisation and total organic carbon (TOC) at different pH values. The kinetics of the AR29 dye decay was followed by high-performance liquid chromatography (HPLC) coupled to a diode array detector (DAD). Carboxylic acids and aromatic compounds formed as by-products of the dye degradation were determined by HPLC-DAD and liquid chromatography coupled to mass spectrometry (LC–MS/MS), respectively. Then, a plausible sequence for AR29 degradation by PEC/EF process was proposed.

2. Experimental procedures

2.1. Chemicals

Acid Red 29 (75% purity), ethylene glycol (99.8% purity), ethanol (⩾99.9% purity), chloroplatinic acid (⩾99.9% purity), heptahydrated ferrous sulphate (⩾99% purity), methanol (⩾99.9% purity) and ammonium fluoride (⩾99.99% purity) were supplied by Sigma–Aldrich. Anhydrous sodium sulphate (⩾99.9% purity) and heptahydrated ferrous sulphate were analytical grade, purchased from Merck. Sulphuric acid, used to regulate the solution pH, was supplied by Sigma–Aldrich. All carboxylic acids were of analytical grade, purchased from Sigma–Aldrich. Standard solutions were prepared with distilled and deionised water (Milli-Q® system, Millipore) with resistivity > 18 MΩ cm at 25 °C.

2.2. Preparation of Pt/TiO_2NT photoelectrodes

Pt/TiO_2NTs photoelectrodes were prepared according to our previous report [2]. Initially, polished titanium sheets from Sigma Aldrich (99.99% purity) were cut (2.5 × 2.0 cm) and ultrasonically degreased in three different solvents (isopropyl alcohol, acetone and ultrapure water) successively for 15 min. The TiO_2 nanotubes (TiO_2NTs) were prepared by anodisation of titanium sheets under potentiostatic conditions [37–39]. For this purpose, a constant potential of 30 V was applied for 50 h using a conventional two-electrode cell, with a titanium sheet as an anode and platinum mesh as a cathode. A glycerol solution containing 0.25 wt% NH_4F and 10 vol% ultrapure water was used as a background electrolyte [40]. After anodisation, TiO_2NTs were fired at 450 °C for 30 min to convert the amorphous TiO_2 to an anatase crystalline phase. Finally, platinum nanoparticles were electrodeposited on the TiO_2-NTs surface using a conventional three-electrode cell, with a platinum mesh as auxiliary electrode and Ag/AgCl as reference electrode. Based on previously obtained results [2], a cathodic current density of 10 mA cm^{-2} was applied for 15 min in an ethanolic solution of 10 mmol L^{-1} chloroplatinic acid for electrodeposition of Pt nanoparticles. All electrochemical assays were performed using a potentiostat/galvanostat (AUTOLAB Model PGSTAT 302) controlled by GPES software.

2.3. Electrolytic systems

All electrochemical experiments were performed in a cylindrical electrochemical cell of 500 mL capacity with a double jacket to maintain the temperature at 25 °C through water recirculation using a thermostat. The anode was the Pt/TiO_2NTs photoelectrode, and the cathode was a carbon–PTFE air-diffusion electrode supplied by E-TEK and assembled as described elsewhere [41]. This cathode was pumped with air (200 mL min^{-1}) to electrogenerate H_2O_2 from O_2 reduction according to reaction (1). The geometric areas of the Pt/TiO_2NTs photoanode and carbon–PTFE air-diffusion cathode were 4.0 cm^2 and 3.0 cm^2, respectively. For all PEC and PEC/EF experiments, a Philips high-pressure Hg lamp (80 W) without glass protection (inserted in a quartz tube) was used as the irradiation source. Both electrodes (i.e., the Pt/TiO_2NTs photoanode and the carbon-PTFE air-diffusion cathode) were arranged around

Table 1
LC–MS/MS identification of chemical structure, retention time and fragment ions of the AR29 dye and aromatic by-products formed during the PEC/EF treatment of AR29 solutions under the optimised conditions described in Fig. 6.

Compound	t_R (min)	Proposed structures	m/z	Fragment ion (MS2) m/z
Acid Red 29 (**1**)	7.14 7.09 7.25	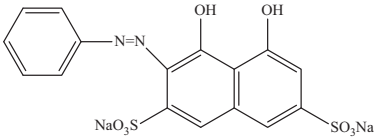	467 $[M-H]^{-a}$ 445 $[M-Na]^{-a}$ 221 $[M-Na]^{2-b}$	– –
4,5-Dihydroxy-6-(phenyldiazenyl)naphthalene-2-sulfonate (**2**)	8.54	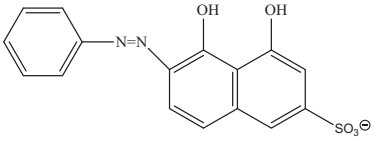	343 $[M-H]^{-a}$	279, 251
Monosodium(trihydroxy-6-(phenyldiazenyl)naphthalene-2,7-disulfonate (**3**)	3.85	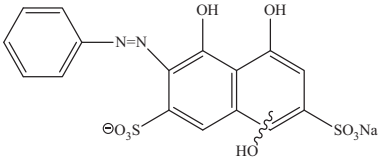	461 $[M-H]^{-a}$	369, 354, 266
Trihydroxy-6-(phenyldiazenyl)naphthalene-2-sulfonate (**4**)	7.17	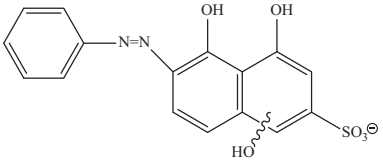	359 $[M-H]^{-a}$	279, 267
Tetrahydroxy-6-(phenyldiazenyl)naphthalene-2-sulfonate (**5**)	7.31	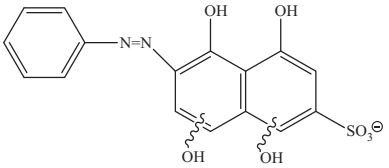	375 $[M-H]^{-a}$	189, 105
Trihydroxy-3-(phenyldiazenyl)-7-sulfonaphthalene-2-sulfonate (**6**)	4.06	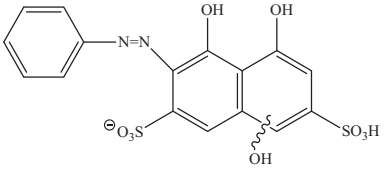	439 $[M-H]^{-a}$	332, 266, 250
6-((Dihydroxyphenyl)diazenyl) exahydroxynaphthalene-2-sulfonate (**7**)	6.45	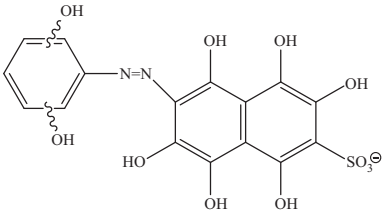	439 $[M-H]^{-a}$	331
2-Amino-4-(3-hydroxypropyl)phenol (**8**)	6.96	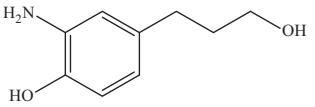	166 $[M-H]^{-a}$	134, 58
6-Hydrazinylbenzene-1,2,3,4,5-pentaol (**9**)	6.10	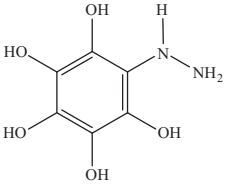	187 $[M-H]^{-a}$	169, 125, 97
2,5-Dihydroxy-4-sulfobenzoic acid (**10**)	7.21	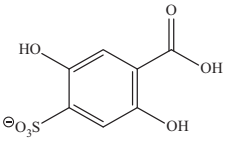	233 $[M-H]^{-a}$	121, 113, 69

(*continued on next page*)

Table 1 (*continued*)

Compound	t_R (min)	Proposed structures	m/z	Fragment ion (MS2) m/z
2,3,4,5,6,7-Hexahydroxynaphthalen-1-olate (**11**)	9.41	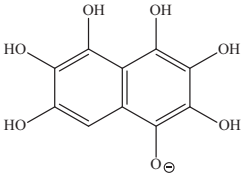	239 $[M-H]^{-a}$	223, 149, 91
4-Carboxy-2,3,6-trihydroxyphenolate (**12**)	7.19	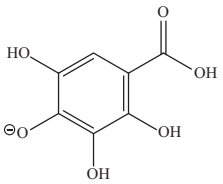	185 $[M-H]^{-a}$	140, 58
2-Carboxybenzoate (**13**)	6.57	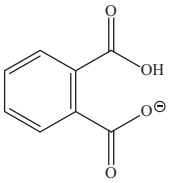	165 $[M-H]^{-a}$	121, 77
Benzoic acid (**14**)	6.09	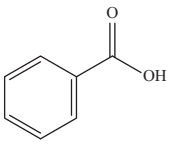	121 $[M-H]^{-a}$	93, 77
Hydroquinone (**15**)	4.71		109 $[M-H]^{-a}$	81
2-(5-Amino-2-hydroxyphenyl)acetic acid (**16**)	6.26	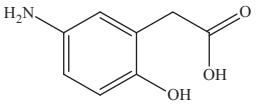	168 $[M+H]^{+c}$	136, 124, 92

[a] Detected in negative mode with $z = 1$.
[b] Detected in negative mode with $z = 2$.
[c] Detected in positive mode with $z = 1$.

the quartz tube, and the gap between Pt/TiO_2NTs and the Hg lamp was ca. 2.0 cm. In the EF experiments, a platinum mesh was used as the anode with the same carbon-PTFE air-diffusion cathode applied in the PEC/EF process but without the Philips high-pressure Hg lamp exposure. The EF and PEC/EF assays were performed in a galvanostatic model with a TECTROL R3/AS1 power supply, and the cell potentials generated during the electrochemical degradation of the AR29 solutions were recorded regularly with a digital multimeter. To establish a comparison with the EF and PEC/EF processes, the photoelectrocatalytic (PEC) experiments were performed using the Pt/TiO_2NTs as photoanode and platinum gauze as cathode for the optimum pH value. The PEC experiments were conducted at a bias potential of 2.0 V *vs.* Ag/AgCl (potentiostatic condition) and using the same lamp previously mentioned.

Comparative EF and PEC/EF treatments of 500 mL of 85.4 mg L^{-1} (35 mg L^{-1} TOC) AR29 solutions in 0.05 mol L^{-1} Na_2SO_4 were performed at pH values in the range of 3.0–6.0. Under the optimised pH value, a photoelectrocatalytic experiment was performed for the same AR29 solution to compare the three studied processes (EF, PEC and PEC/EF). All electrochemical assays were conducted under continuous stirring with a magnetic bar to promote the transport of active species towards the electrodes.

2.4. Instruments and analytical procedures

The morphology and composition of Pt/TiO_2NTs photoelectrodes were analysed by X-ray diffraction (XRD) using a Siemens D5000 system (DIFFRAC PLUS XRD Commander) with a Cu kα radiation and Field Emission Gun-Scanning Electron Microscopy (FEG-SEM) of high resolution with the source of electrons by field emission model JSM-7500F. The photoactive properties of Pt/TiO_2NTs electrodes were evaluated by diffuse reflectance spectroscopy (DRS) and linear sweep voltammetry (photocurrent) measurements. All characterisations mentioned above are described elsewhere in detail [2].

The electrogenerated hydrogen peroxide was determined using a spectrophotometric method based on the reaction between H_2O_2 and ammonium metavanadate in acid medium and detailed in the work of Paterlini et al. [42]. Basically, this reaction forms a red–orange solution corresponding to the peroxovanadium cation (VO_3^+) with its maximum absorbance at $\lambda = 450$ nm.

The decolourisation of AR29 dye solutions was monitored based on the absorbance decay at 508 nm (wavelength of maximum AR29 absorption) using a Hewlett Packard 8453 UV–Vis spectrophotometer. The decolourisation efficiencies were calculated using Eq. (7) [9]:

$$\text{Decolourisation efficiency}/\% = [(A_0 - A_t)/A_0 0] \times 100 \quad (7)$$

where A_0 and A_t are the maximum absorbance ($\lambda = 508$ nm) at the initial time and time t, respectively.

Total organic carbon (TOC) measurements were performed to evaluate the mineralisation efficiencies (TOC abatement) of AR29 solutions via EF, PEC and PEC/EF processes and by using a Shimadzu TOC-V CPN analyser. The AR29 decay was followed by

reversed-phase HPLC using a Shimadzu 10 Avp LC fitted with a Spherisorb ODS2 5 μm (150 mm × 4.6 mm) column at 35 °C and coupled with a photodiode array detector selected at λ = 508 nm. In these kinetics studies, a 75:25 (v/v) acetonitrile/phosphate buffer mixture at pH 3.5 and a flow rate of 0.6 mL min^{-1} was used as mobile phase.

The aromatic compounds formed during the AR29 dye degradations were determined by LC/MS/MS analysis in a High Performance Liquid Chromatography of 1200 Agilent Technologies coupled to a Mass Spectrometer 3200 QTRAP (Linear Ion Trap Quadrupole LC/MS/MS Mass Spectrometer), AB SCIEX Instruments operating in a negative mode and TurbolonSpray ionisation. *Full-scan* and fragment ion experiments were performed using the following parameters: curtain gas: 10 psi, Ion Spray: −4500 V, Gas 1: 50 psi, Gas 2: 50 psi, Temperature: 450 °C, Declustering Potential: −40.00 V, Entrance Potential: −4.50 V and Interface heater: ON. The collision energy used to fragment ion experiments ranged from 20.0 to 35.0 V. The LC analyses were performed using an Agilent Zorbax C-18 5.0 μm (150 mm × 4.6 mm) column at 25 °C fitted to a C18 column guard. The mobile phase was water containing 0.01% formic acid and methanol in a gradient elution from 5% to 100% methanol in 15 min. The flow used was 1.0 mL min^{-1}, and the injection volume was 25 μL. The samples were also analysed in a positive mode, using Ion Spray: 5500 V, Declustering Potential: 50.0 V and Entrance Potential: 10.0 V; the others parameters were the same as the ones used in negative mode.

For the LC–MS/MS analysis, aliquots of 2.5 mL of the electrolysed dye solutions were withdrawn at predetermined times. These samples were extracted using a solid-phase cartridge (Strata X polymeric cartridge) previously conditioned with 3.0 mL methanol and balanced with 3.0 mL ultra-pure water. Subsequently, the samples were cleaned up by the conditioned cartridge and eluted with a mobile phase consisting of a 50:50 (v/v) methanol/water mixture with formic acid 0.1% (v/v). Then, 25.0 μL of each sample was injected.

The carboxylic acids generated were detected and identified by ion-exclusion using the same HPLC mentioned above with a Rezex ROA-Organic Acid 8 μm (300 mm × 7.8 mm) column coupled with a photodiode array detector selected at λ = 210 nm. The mobile phase used for the carboxylic acids was 4.0 mmol L^{-1} H_2SO_4 at 0.6 mL min^{-1}.

3. Results and discussion

3.1. Hydrogen peroxide electrogeneration

Considering that the performance of electro-Fenton processes is directly dependent on the H_2O_2 electrogeneration onto the cathode surface from reaction (1), the ability of the carbon–PTFE air-diffusion cathode to produce H_2O_2 in the EF and PEC/EF processes applied in this work was evaluated. Fig. 1 compares the ability of an undivided cell to produce H_2O_2 in 100 mL of 0.05 mol L^{-1} Na_2SO_4 (pH = 3.0) at a current density of 16.67 mA cm^{-2} for 420 min of electrolysis for both EF and PEC/EF processes. As shown in Fig. 1, the concentration of H_2O_2 increases gradually with electrolysis time in both conditions to achieve plateau concentrations above 300 min. Maximum H_2O_2 concentrations of 65.3 and 94.0 mg L^{-1} were achieved for the PEC/EF and EF processes, respectively. These roughly stationary H_2O_2 concentrations achieved for longer electrolysis times in both conditions are evidence that the electrogeneration and destruction of H_2O_2 become equal [13].

Although the maximum H_2O_2 accumulation has been achieved by electrolysis without UV–Vis irradiation exposure (EF process), the degradation experiments conducted with this irradiation source (PEC/EF process) were more efficient for the AR29 dye mineralisation, as will be discussed below. The smaller concentration of hydrogen peroxide accumulated for the PEC/EF assay can be related to the action of UV irradiation, which promotes the homolytic cleavage of H_2O_2 according to reaction (6) [43].

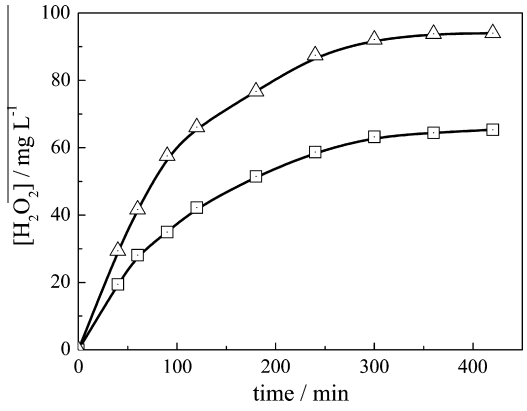

Fig. 1. Concentration of H_2O_2 produced in the air-diffusion cathode from reaction (1) by electrolysing 100 mL of 0.05 mol L^{-1} Na_2SO_4 solutions (pH = 3.0) at a current density of 16.67 mA cm^{-2} during 420 min of electrolysis for the (□) EF and (△) PEC/EF processes. Irradiation source used in the PEC/EF process: Philips high-pressure Hg lamp (80 W).

The hydrogen peroxide decomposition using the UV–Vis irradiation source can also be caused by two photoelectrochemical processes on the Pt/TiO_2NTs surface: (i) H_2O_2 reduction by the electron photogenerated in the conduction band (CB) in the semiconductor by reaction (8) [22,44] and (ii) the reaction between H_2O_2 and the superoxide radical $\cdot O_2^-$ (formed after the preadsorbed O_2 molecules to trap electrons in the conduction band) by the anodic reaction (9) [44]:

$$H_2O_2 + eCB^- \rightarrow \cdot OH + OH^- \quad (8)$$

$$H_2O_2 + \cdot O_2^- \rightarrow \cdot OH + OH^- + O_2 \quad (9)$$

These reactions and other secondary reactions may have contributed (even if in small proportions) to the consumption of hydrogen peroxide and simultaneously to the degradation of organic contaminants. The influence of hydrogen peroxide on the AR29 degradation for both Fenton processes will be discussed in more detail in the following subsections. However, when produced in excess, the hydrogen peroxide acts as ·OH and hole (h^+) scavengers to form the hydroperoxyl radical from reactions (10) and (11) [44,45], reducing the degradation rate of the AR29 dye in the PEC/EF process applied in this work.

$$\cdot OH + H_2O_2 \rightarrow + H_2O + HO_2^{\cdot} \quad (10)$$

$$H_2O_2 + h^+ \rightarrow H^+ + HO_2^{\cdot} \quad (11)$$

3.2. Decolourisation and mineralisation of AR29 dye by PEC, EF and PEC/EF processes

To comparatively evaluate the efficiency of the PEC, EF and PEC/EF processes on the decolourisation and degradation rates of 85.4 mg L^{-1} AR29 solutions in 0.05 mol L^{-1} Na_2SO_4, a conventional electrochemical cell was used. Based on our previous reports [10], for the EF and PEC/EF processes, 0.5 mmol L^{-1} Fe^{2+} was added as catalyst. First, comparative EF and PEC/EF treatments were performed at pH values in the range of 3.0 to 6.0. This pH range was chosen considering the relation of the surface charge of TiO_2NTs (isoelectric point – IEP), the acid dissociation constant (pk_a) of AR29 and the optimum pH of approximately 3.0 for Fenton's

reaction (2) [34], as will be explained below. Additionally, basic pH values were not studied to avoid the precipitation of iron species, thus limiting the Fenton's reaction (2). Then, for the optimal pH value, degradation assays were performed for the same AR29 solution to compare the three processes (EF, PEC and PEC/EF) studied. In all degradation assays, slight pH decreases with prolonged degradation time were observed, most likely due to the formation of organic acid compounds such as aliphatic carboxylic acids [9,34]. The EF PEC/EF treatments were conducted in galvanostatic mode due to the efficient H_2O_2 electrogeneration achieved when compared to the assays conducted in potentiostatic conditions.

Fig. 2 compares the decolourisation efficiencies (calculated from Eq. (7)) for 85.4 mg L^{-1} of AR29 solutions treated by EF and PEC/EF processes at pH values of 3.0, 4.5 and 6.0 and applying a current density of 16.67 mA cm^{-2} during 60 min of electrolysis. Total decolourisation was achieved for both the EF and PEC/EF processes after 60 min of electrolysis at pH 3.0 and 4.5. However, at pH 6.0, the decolourisation efficiencies reached only 84% and 92% for the EF and PEC/EF processes, respectively.

The total decolourisation obtained for more acidic pH values was most likely due to the favouring of the Fenton's reaction (2), which enhances the production of ·OH in the bulk solution in this experimental condition [10,34]. The other factor that also favoured the total decolourisation process was the better adsorption process of the ionic form of the AR29 ($AR29^{2-}$) onto the Pt/TiO_2NTs photoelectrode surface in more acidic conditions, which is considered as the first step in the photoelectrocatalytic oxidation of the AR29 dye [2,46]. Considering the acid dissociation constant value for the AR29 dye ($pK_a = -3.08$ at 25 °C), the ionic form of the dye ($AR29^{2-}$) predominates in the pH range studied [2]. Furthermore, according to the literature, the IEP for TiO_2 (i.e., the pH value at which the surface charge is electrically neutral) is approximately 5.4–6.0 [47–49]. Thus, at pH ⩽ 4.5, the surface of TiO_2NTs would be positively charged due to the protonation of Ti–OH bonds according to reaction (12). At pH ⩾ 6, the opposite behaviour (surface negatively charged) is observed, as described in reaction (13) [48].

$$\text{pH} < \text{IEP}: \ \text{Ti} - \text{OH} + \text{H}^+ \rightarrow \text{Ti} - \text{OH}_2^+ \quad (12)$$

$$\text{pH} > \text{IEP}: \ \text{Ti} - \text{OH} + \text{OH}^- \rightarrow \text{Ti} - \text{O}^- + \text{H}_2\text{O} \quad (13)$$

Therefore, the adsorption process of the $AR29^{2-}$ onto the TiO_2-NTs surface is gradually suppressed with increasing pH values, which decreases the photoelectrocatalytic efficiency of the Pt/TiO_2-NTs photoanode. This behaviour indicates that the kinetics of AR29 oxidation is favoured under more acidic conditions (see Fig. 2). Furthermore, the decolourisation efficiency was also reduced when the pH varied from 3.0 to 6.0 due to the partial precipitation of Fe^{3+} and its slower reduction to Fe^{2+}, suggesting inefficient production of ·OH in the bulk solution of Fenton's reaction (2) for higher pH values [9].

When comparing the decolourisation efficiencies for the EF and PEC/EF processes (see Fig. 2), it can be observed that the AR29 dye was more slowly decolourised by the EF process. The faster decolourisation of AR29 solutions promoted by the PEC/EF process is attributed mainly to the additional ·OH production due to water oxidation by the holes generated on the photoanode surface [2] by the photolytic cleavage of H_2O_2 from reaction (6) [22,43,45] and by the photochemical reduction of $Fe(OH)^{2+}$ complexes according to reaction (5) [9,20,21]. In addition, the hydrogen peroxide may also have increased the mineralisation efficiency of the AR29 solution by using the efficiency of the PEC/EF process due to the inhibition of the electron/hole pair recombination onto the photoanode surface with the additional generation of ·OH radicals according to the photochemical reactions (8) and (9) [22,44,50].

Fig. 3 illustrates the effect of pH value on TOC abatement of the 84.5 mg L^{-1} AR29 solutions treated by EF and PEC/EF processes at pH values of 3.0, 4.5 and 6.0 and a current density of 16.67 mA cm^{-2} during 120 min of electrolysis. The TOC values decayed more rapidly for the PEC/EF process compared to EF. For the PEC/EF process, TOC reductions of 97%, 93% and 86% after 120 min electrolysis were obtained for pH values of 3.0, 4.5 and 6.0, respectively. However, when applied to the EF process, only 89%, 82% and 72% TOC abatement were achieved (after 120 min electrolysis) for pH values of 3.0, 4.5 and 6.0, respectively. These TOC abatement values obtained for both processes qualitatively corroborate the decolourisation assays (see Fig. 2), where the maximum efficiencies of decolourisation and TOC abatement were achieved for the PEC/EF process at pH 3.0. This behaviour also suggests that the highest mineralisation efficiencies obtained for the PEC/EF process could be due to the additional production of ·OH, as previously discussed.

To evaluate the contribution of each process, the degradation of AR29 solutions by the EF and PEC/EF processes was compared to the PEC process at pH 3.0 (optimum pH value), applying the same charge per unit volume of the dye solutions in all assays (200 mA h L^{-1}). In both Fenton processes (EF and PEC/EF), 16.67 mA cm^{-2} was applied. However, the PEC treatment was conducted at a constant potential of 2.0 V *vs.* Ag/AgCl (KCl 3.0 mol L^{-1})

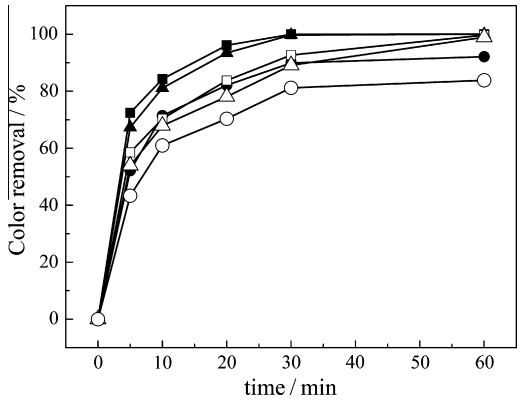

Fig. 2. Effect of pH on colour removal *vs.* degradation time of 500 mL of a 85.4 mg L^{-1} Acid Red (AR29) solution in 0.05 mol L^{-1} Na_2SO_4 with 0.5 mmol L^{-1} Fe^{2+} and applying a current density of 16.67 mA cm^{-2} for: (□, Δ, ○) EF and (■, ▲, ●) PEC/EF processes. Applied pH: (■, □) 3.0, (▲, △) 4.5 and (●, ○) 6.0. Irradiation source used in the PEC/EF process: Philips high-pressure Hg lamp (80 W).

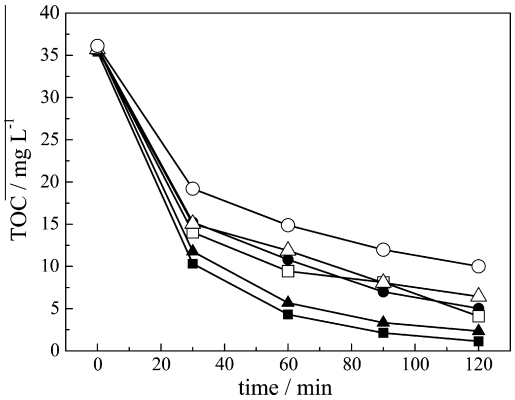

Fig. 3. Effect of pH on TOC abatement *vs.* degradation time of 500 mL of a 85.4 mg L^{-1} Acid Red (AR29) solution in 0.05 mol L^{-1} Na_2SO_4 with 0.5 mmol L^{-1} Fe^{2+} and applying a current density of 16.67 mA cm^{-2} for: (□, △, ○) EF and (■, ▲, ●) PEC/EF processes. Applied pH: (■, □) 3.0, (▲, △) 4.5 and (●, ○) 6.0. Irradiation source used in the PEC/EF process: Philips high-pressure Hg lamp (80 W).

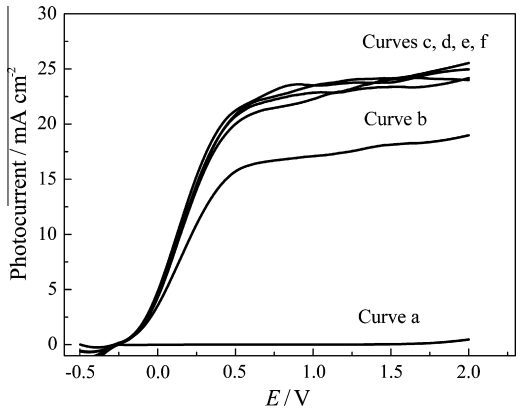

Fig. 4. Photocurrent (linear sweep voltammetry) measurements obtained for TiO_2NTs (Curve b) and Pt/TiO_2NTs (Curves a and c–f) photoelectrodes at 10 mV s^{-1} and in 0.100 mol L^{-1} Na_2SO_4. Photocurrent for Curve a in the absence of UV–Vis lamp exposure.

based on the photocurrent assays illustrated in Fig. 4. As observed in Fig. 4 (see Curves c, d, e and f for the Pt/TiO_2NTs), the photocurrent values reach plateaus (saturated states) in the potential range of 1.0 to 2.0 V, justifying the choice of the potential of 2.0 V for the PEC assay. Then, the photoelectrochemical stability of the Pt/TiO_2NTs electrodes was evaluated after four PEC/EF treatments through 6 h electrolysis for each assay (Fig. 4 – Curves c, d, e and f). By comparing these assays, it can be observed that the photocurrent values do not vary significantly, demonstrating that the Pt/TiO_2NTs electrode showed good stability. Curve a shows the photocurrent obtained in the absence of light exposure, and Curve b shows the photocurrent for the TiO_2NTs (undecorated) under UV light exposure, respectively. As expected, Curve a shows that no photocurrent was generated. Comparing the photocurrent obtained for the undecorated photoanode (Curve b) with the decorated one (Curves c, d, e and f), it is possible to observe that the photocurrent generated for the Pt/TiO_2NTs (decorated) photoelectrode (Curves c–f) are higher than the TiO_2NTs one. These results show that the decoration of TiO_2NTs with Pt nanoparticles promotes efficient light absorption and reduces the recombination of the photogenerated electron–hole pairs generated under UV light exposition, improving the photoelectrocatalytic performance of the semiconductor.

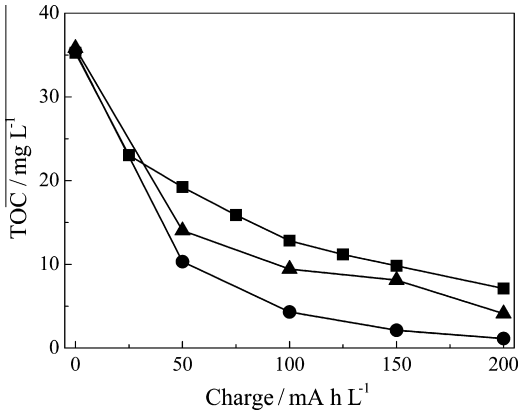

Fig. 5. Comparative TOC abatement *vs.* applied electric charge of 500 mL of 85.4 mg L^{-1} Acid Red (AR29) solutions in 0.05 mol L^{-1} Na_2SO_4 at pH 3.0 for the: (■) PEC, (▲) EF and (●) PEC/EF processes. In the EF and PEC/EF processes, 0.5 mmol L^{-1} Fe^{2+} was added to the solution, and a current density of 16.67 mA cm^{-2} was applied. For the PEC treatment, a constant potential of 2.0 V *vs.* Ag/AgCl (KCl 3.0 mol L^{-1}) was applied. Irradiation source used in the PEC and PEC/EF processes: Philips high-pressure Hg lamp (80 W).

Fig. 5 compares the degradation performance of the 85.4 mg L^{-1} AR29 solutions in 0.05 mol L^{-1} Na_2SO_4 and with 0.5 mmol L^{-1} Fe^{2+} as catalyst for the EF and PEC/EF processes. From this comparative analysis, it can be observed that the mineralisation ability of AR29 solutions for all EAOPs increased in the sequence PEC < EF < PEC/EF. By applying electric charges per unit volume of dye solutions of 200 mA h L^{-1}, TOC reductions of 81%, 90% and 98% were obtained for the PEC, EF and PEC/EF processes, respectively (Fig. 5).

In the PEC process, the degradation of the AR29 dye is promoted basically by direct oxidation in the holes (formed at the valence band) and by the ·OH radicals generated after water oxidation by holes on the Pt/TiO_2NTs surface [2]. At higher concentrations, the light intensity reaching the semiconductor surface is reduced due to the lower transparency of the solution [51].

In the EF process, the AR29 dye is mineralised mainly by the action of ·OH radicals formed from Fenton's reaction (2) occurring continuously in the bulk solution [9–11,34]. Thus, the AR29 dye is more rapidly degraded by the EF process than by the PEC, possibly due to the absence of mass transfer limitations in the EF process. In other words, in the EF process, the dye is mineralised in the solution, whereas for the PEC process, the target compounds must be conducted onto the anode surface for oxidisation. These different paths of oxidation explain why the EF process was almost 10% more efficient than the PEC process for TOC abatement for the same applied electric charge (see Fig. 5).

Finally, the higher TOC abatement obtained for the PEC/EF process in comparison with the PEC and EF processes is credited to the additional production of ·OH by the photolytic reactions (5) and (6) in the bulk solution and from reactions (8) and (9) onto the Pt/TiO_2NTs surface, as stated above. Furthermore, the photolysis of Fe(III)–carboxylate complexes by reaction (4) enhanced the degradation efficiency [9–11,18–21,34,41].

3.3. Degradation kinetics of the AR29 dye

The degradation of AR29 solutions during the three EAOP treatments (PEC, EF and PEC/EF) at pH 3.0 were followed by reverse-phase HPLC coupled to a diode array detector. The recorded chromatograms displayed a well-defined peak at a retention time (t_R) of 8.35 min, which was ascribed to the AR29 dye. Direct photolysis of the AR29 dye was discarded because its concentration in solution showed an insignificant decrease after 60 min electrolysis under UV–Vis lamp exposition.

Fig. 6 compares the removal of the AR29 dye by the PEC, EF and PEC/EF processes under the same conditions described in Fig. 5. As can be observed in Fig. 6, for all treatments, progressive destruction of AR29 was obtained, with an increasing oxidation rate in the sequence PEC < EF < PEC/EF, consistent with the findings from the TOC decays. The higher oxidation capability shown by the coupled PEC/EF process in comparison with the single systems (i.e., PEC and EF processes) clearly indicates the synergistic effect from the photocatalytic reduction of the electrogenerated H_2O_2 from the reaction (8) [22,44] onto the electrode surface, minimising the electron/hole pair recombination onto the photoanode surface with concomitant ·OH production and transference of photo-electrons to the air-diffusion cathode, (ii) an additional production of ·OH according to the photocatalytic reactions (5) [9,20,21] and (6) [43] in the bulk solution and onto the Pt/TiO_2NTs surface from reaction (9) [44] and (iii) the photolysis of Fe(III)–carboxylate complexes formed as degradation products by reaction (4) [9–11,18–21,34,37]. Fig. 6 also shows that the AR29 dye completely disappears using applied charges of only 13, 16 and 20 mA h L^{-1} for the PEC, EF and PEC/EF processes, respectively.

The kinetic of degradation of AR29 solution during the PEC/EF treatment is illustrated in Fig. 7. As shown, the AR29 concentration decayed continuously until it disappeared at 7.0 min of electroly-

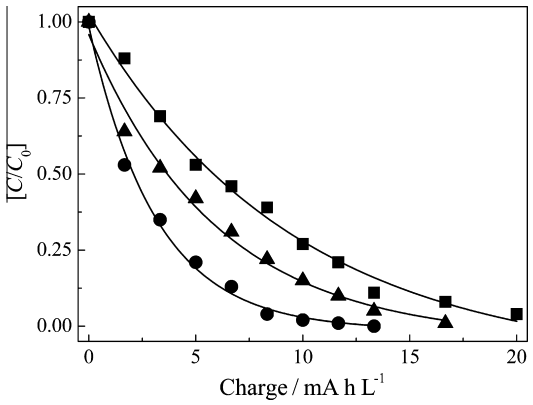

Fig. 6. Normalised AR29 concentration decay *vs.* applied electric charge of 500 mL of 85.4 mg L^{-1} Acid Red (AR29) solutions for the: (■) PEC, (▲) EF and (●) PEC/EF processes and under the same conditions described in Fig. 5. Chromatographic conditions: mobile phase 75:25 (v/v) acetonitrile/phosphate buffer (pH 3.5) and flow rate of 0.6 mL min^{-1}.

sis. The inset of the Fig. 7 highlights the good linear correlations obtained considering pseudo first-order kinetics for the AR29 concentration decays in the PEC/EF treatment, suggesting an attack of constant amounts of the oxidant ·OH (in the bulk and on the anode surface), at least at the beginning of the degradation experiments [9–11]. From this analysis, a pseudo first-order constant (k_1) of 11.0×10^{-3} s^{-1} ($R^2 = 0.990$) was found for the PEC/EF process. The fast AR29 removal compared with the slow TOC abatement could be attributed to the formation of persistent organic by-products during the PEC/EF treatment [9].

3.4. Identification of oxidation products

It is well known that during EAOP processes, various by-products can be formed during the mineralisation of organic compounds, i.e., up to their transformation into CO_2, water and inorganic ions [10]. In this context, aromatic and aliphatic intermediates formed during the PEC/EF treatment of AR29 solutions were identified by LC–MS/MS and HPLC techniques, respectively.

Table 1 lists the identification of the target AR29 dye and its main degradation products revealed by *m*/*z* transition detected in the negative mode. The results indicate that the AR29 dye presented a well-defined peak with *m*/*z* 439 before the PEC/EF treatment. In the sequence, LC–MS/MS spectra presented the following products assigned as compounds 2–16 in Table 1. The products identified as compounds **2** and **3** after 5 min electrolysis were generated by desulphonation and hydroxylation of the initial compound **1**, respectively. Successive hydroxylations of **2** formed the compounds **4**, **5** and **7**, whereas the hydroxylation of **3** yielded compound **6**. Compounds **4** to **7** were detected between 15 and 20 min of electrolysis. The hydroxylation of **3** followed by a desulphonation reaction could also favour the formation of **4**, and the hydroxylation and desulphonation of **6** yields compound **7**. The cleavage of —N=N— bonds of the aromatic compounds **4** and **7,** identified only after 20 min of electrolysis, led to the formation of the benzenic compounds **8**–**10** and naphthalenic compound **11**, respectively. These compounds (**8**–**11**) were oxidised to other benzenic products (compounds **12**–**16**). Further oxidations lead to the formation of aliphatic products such as carboxylic acids **17**–**18**, possibly by the cleavage of the benzenic rings (oxidative ring opening reactions) of the aromatic by-products. The by-products **12**–**18** were only detected after 30–40 min electrolysis.

The final product was also analysed using ion-exclusion chromatograms of the electrolysed AR29 solutions by the PEC/EF process. The chromatograms revealed the generation of carboxylic acids such as succinic (t_r = 11.3 min) and oxalic (t_r = 5.2 min) acid, which were degraded until their total mineralisation [8,10,11,41]. Other carboxylic acids such as oxalacetic, tartronic, tartaric, malonic and fumaric are expected to be generated from the oxidation/cleavage of the aromatic rings of azo dyes [10].

In the EF and PEC/EF processes, carboxylic acids are present in solution as Fe(III)–carboxylate complexes, which can be photolysed when exposed to the UV–Vis lamp in the PEC/EF process [10].

3.5. Proposed AR29 degradation sequence

Based on the aromatic and aliphatic intermediates formed as by-products during the PEC/EF treatment of AR29 and detected by LC–MS/MS (see Table 1) and HPLC, a plausible mineralisation pathway for the PEC/EF degradation of AR29 is proposed in Fig. 8. In this proposed AR29 degradation sequence, the main oxidising agents ·OH and M(·OH) are considered, which are formed in the bulk and on the Pt/TiO_2NTs surface. However, other weaker oxidants (e.g., $HO_2^{\cdot}$, O_3) can also be generated during the PEC/EF treatment, albeit in smaller proportions [10].

According to the results presented in Fig. 8, the mineralisation of the AR29 (**1**) dye due to the attack of the oxidising agents may have been initiated by two paths: (i) desulphonation in the naphthalenic ring on the C(6)-position, which leads to the formation of **2** (path A), and (ii) successive hydroxylations to form compounds **3** and **6** (path B). Compound **4** can be formed from the hydroxylation reaction of **2** or from the desulphonation of **3**. Consecutive hydroxylations of **4** lead to the formation of compounds **5** and **7**. Compound **7** can also be formed from successive hydroxylations and from desulphonation of **6**. The oxidation of **7** leads to the cleavage of the C–N bond, which is subsequently either oxidised to **10** or hydroxylated and desulphonated to yield the benzenic compound **9** and the naphthalenic compound **11**. The degradation of the naphthalenic compound **11** with ring opening leads to the formation of the benzenic compounds **12**–**15**. Compound **4** can even be oxidised to generate **8** and **16** after desulphonation and cleavage of the —N=N— bond. Further oxidation of the benzenic compounds **8**–**10** and **12**–**16** with ring opening leads to the formation of the aliphatic acids **17**–**18**. These carboxylic acids can be further oxidised to ultimate acids such as formic, oxalic and oxamic acid, forming Fe(III)–carboxylate complexes, which can be photolysed by UV–Vis radiation [10,20,41].

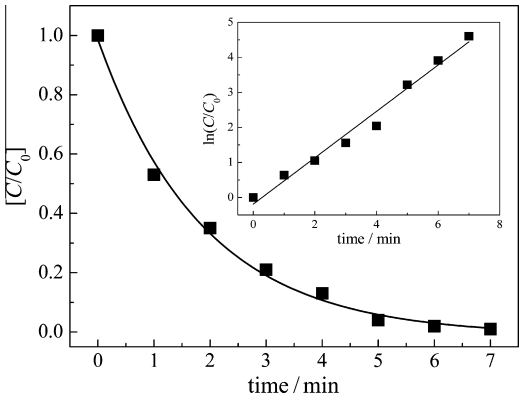

Fig. 7. Normalised AR29 concentration decay *vs.* degradation time during the PEC/EF treatment of 500 mL of 85.4 mg L^{-1} Acid Red (AR29) solution in 0.05 mol L^{-1} Na_2SO_4 with 0.5 mmol L^{-1} Fe^{2+} (pH = 3.0), applying a current density of 16.67 mA cm^{-2} and under UV–Vis lamp exposure. The inset panel presents the kinetic analysis assuming a pseudo first-order reaction for the AR29 dye degradation. Chromatographic conditions: mobile phase 75:25 (v/v) acetonitrile/phosphate buffer (pH 3.5) and flow rate of 0.6 mL min^{-1}.

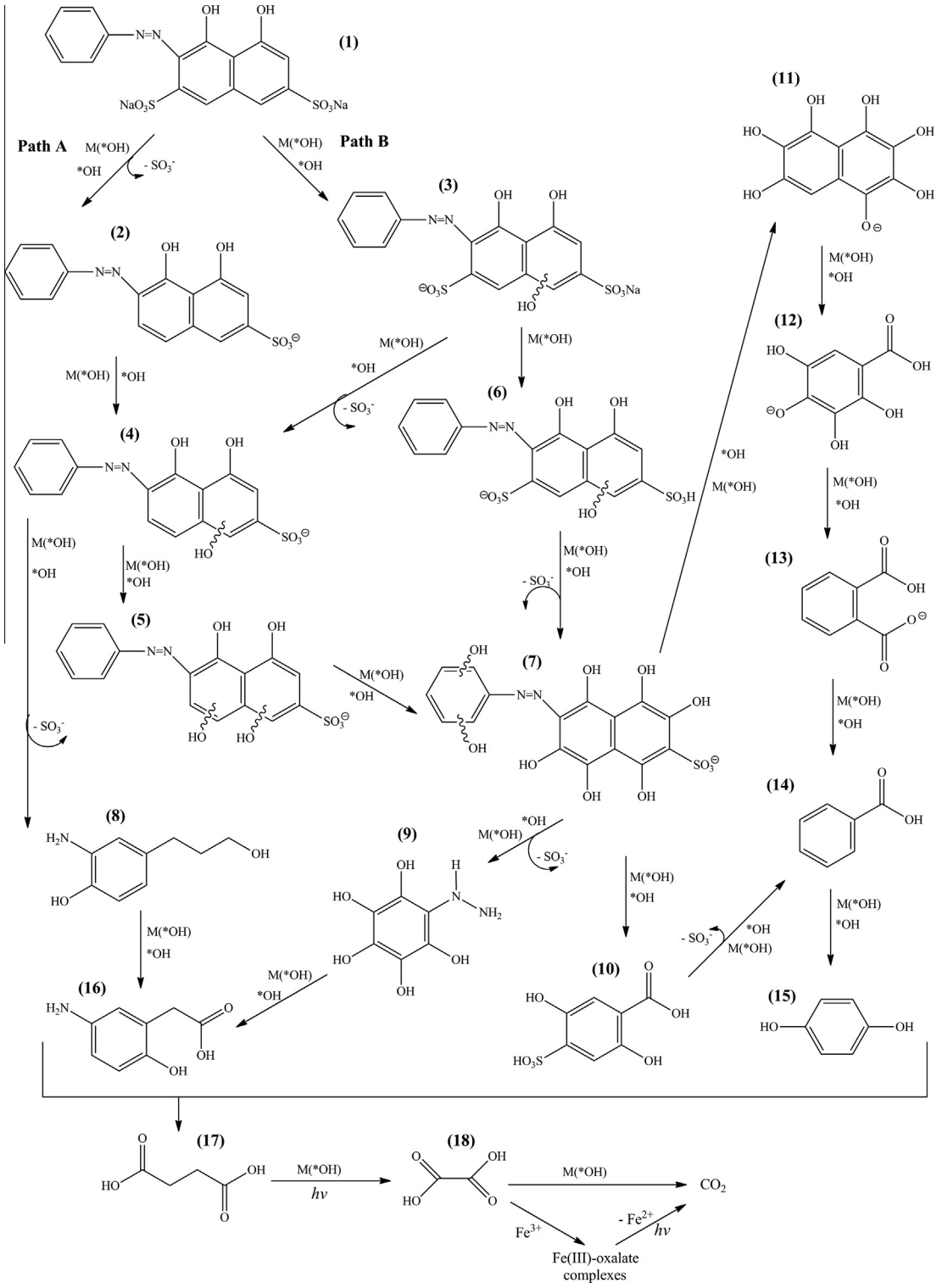

Fig. 8. General pathway proposed for AR29 degradation by PEC/EF process under the same conditions described in Fig. 7.

Total mineralisation of the AR29 dye was most likely prevented by the formation of persistent organic pollutants such as N-derivatives and other undetected aromatic compounds, which cannot be mineralised by ·OH and UV–Vis radiation [10].

4. Conclusion

In this study, the discolouration and mineralisation of the AR29 dye were comparatively investigated by PEC, EF and PEC/EF processes. From this comparative analysis, it was concluded that the mineralisation ability of the dye solutions increased in the sequence PEC < EF < PEC/EF with TOC decays of 81%, 90% and 98%, respectively. For the PEC/EF process, the AR29 decays followed a pseudo first-order kinetic, suggesting constant ·OH and M(·OH) production, at least at the beginning of the treatments. The higher mineralisation capacity obtained for the PEC/EF process in comparison with the PEC and EF processes was ascribed to the additional production of ·OH by the photolytic reactions in the bulk

solution and on the Pt/TiO_2NTs surface. The synergetic effect of the photocatalytic reduction of H_2O_2 on the electrode surface (which minimises the electron/hole pair recombination) and the photolysis of Fe(III)–carboxylate complexes also enhanced the degradation efficiency of the coupled PEC/EF process. For the PEC/EF process at the optimum pH value 3.0, the aromatic and aliphatic by-products were identified by LC–MS/MS and HPLC, respectively. Finally, a plausible pathway for the AR29 dye degradation via the PEC/EF process was proposed based on the by-products detected by HPLC and LC–MS/MS. Total mineralisation of the AR29 dye was prevented, most likely by the formation of persistent organic by-products. Finally, these results revealed that the coupling of electrochemical methodologies is a promising approach for the remediation of effluents containing textile dyes.

Conflict of interest

There is no conflict of interest.

Acknowledgements

The authors are grateful to the Brazilian research funding agencies CNPq, CAPES and FAPESP (Process: 2011/21606-9) for financial support.

References

[1] Q. Chen, H. Liu, Y. Xin, X. Cheng, Chem. Eng. J. 241 (2014) 145–154.
[2] L.C. Almeida, M.V.B. Zanoni, J. Braz. Chem. Soc. 25 (2014) 579–588.
[3] G.G. Bessegato, J.C. Cardoso, B.F. Silva, M.V.B. Zanoni, J. Photochem. Photobiol. A 276 (2013) 96–103.
[4] K. Rajeshwar, M.E. Osugi, W. Chanmanee, C.R. Chenthamarakshan, M.V.B. Zanoni, P. Kajitvichyanukul, R. Krishnan-Ayer, J. Photochem. Photobiol. C 9 (2008) 171–192.
[5] G.F. Pereira, R.C. Rocha-Filho, N. Bocchi, S.R. Biaggio, Chem. Eng. J. 198–199 (2012) 282–288.
[6] S. Garcia-Segura, F. Centellas, C. Arias, J.A. Garrido, R.M. Rodríguez, P.L. Cabot, E. Brillas, Electrochim. Acta 58 (2011) 303–311.
[7] S. Trabelsi, N. Oturan, N. Bellakhar, M.A. Oturan, J. Mater. Environ. Sci. 3 (2012) 426–433.
[8] F.C. Moreira, S. Garcia-Segura, V.J.P. Vilar, R.A.R. Boaventura, E. Brillas, Appl. Catal. B: Environ. 142–143 (2013) 877–890.
[9] L.C. Almeida, S. Garcia-Segura, C. Arias, N. Bocchi, E. Brillas, Chemosphere 89 (2012) 751–758.
[10] L.C. Almeida, S. Garcia-Segura, N. Bocchi, E. Brillas, Appl. Catal. B: Environ. 103 (2011) 21–30.
[11] S. Garcia-Segura, L.C. Almeida, N. Bocchi, E. Brillas, J. Hazard. Mater. 194 (2011) 109–118.
[12] A.R.F. Pipi, I. Sirés, A.R. Andrade, E. Brillas, Chemosphere 109 (2014) 49–55.
[13] B.R. Garza-Campos, J.L. Guzmán-Mar, L.H. Reyes, E. Brillas, A. Hernández-Ramírez, E.J. Ruiz-Ruiz, Chemosphere 97 (2014) 26–33.
[14] C.-C. Su, A.-T. Chang, L.M. Bellotindos, M.-C. Lu, Sep. Purif. Technol. 99 (2012) 8–13.
[15] F.E.F. Rêgo, A.M.S. Solano, I.C.C. Soares, D.R. Silva, C.A. Martinez-Huitle, M. Panizza, J. Environ. Chem. Eng. 2 (2014) 875–880.
[16] M. Panizza, M.A. Oturan, Electrochim. Acta 56 (2011) 7084–7087.
[17] A. Wang, Y.Y. Li, J. Ru, J. Chem. Technol. Biotechnol. 85 (2010) 1463–1470.
[18] Y. Sun, J.J. Pignatello, Environ. Sci. Technol. 27 (1993) 304–310.
[19] I. Sirés, J.A. Garrido, R.M. Rodríguez, E. Brillas, N. Oturan, M.A. Oturan, Catal. B: Environ. 72 (2007) 382–394.
[20] S. Garcia-Segura, E. Brillas, Water Res. 45 (2011) 2975–2984.
[21] Y. Zuo, J. Hougné, Environ. Sci. Technol. 26 (1992) 1014–1022.
[22] M. Saquib, M.A. Tariq, M.M. Haque, M. Muneer, J. Environ. Manage. 88 (2008) 300–306.
[23] A.R. Khataee, M. Safarpour, A. Naseri, M. Zarei, J. Electroanal. Chem. 672 (2012) 53–62.
[24] M. Zarei, A.R. Khataee, R. Ordikhani-Seyedlar, M. Fhatinia, Electrochim. Acta 55 (2010) 7259–7265.
[25] X. Ding, Z. Ai, L. Zhang, J. Hazard. Mater. 239–240 (2012) 233–240.
[26] T.T. Guaraldo, S.H. Pulcinelli, M.V.B. Zanoni, J. Photochem. Photobiol. A 217 (2011) 259–266.
[27] H. An, J. Zhou, J. Li, B. Zhu, S. Wang, S. Zhang, S. Wu, W. Huang, Catal. Commun. 11 (2009) 175–179.
[28] A. Kar, Y.R. Smith, V. Subramanian, Environ. Sci. Technol. 43 (2009) 3260–3265.
[29] L. Xiang, X. Zhao, C. Shang, J. Yin, J. Colloid Interf. Sci. 403 (2013) 22–28.
[30] K. Xie, L. Sun, C. Wang, Y. Lai, M. Wang, H. Chen, C. Lin, Electrochim. Acta 55 (2010) 7211–7218.
[31] R. Asahi, Y. Taga, W. Mannstadt, A.J. Freeman, Phys. Rev B: Condens. Matter. 61 (2000) 7459–7465.
[32] M.F. Brugnera, C.Q.F. Leite, M. Miyata, M.V.B. Zanoni, Water Res. 47 (2013) 6596–6605.
[33] P. Christopher, D.B. Ingram, S. Linic, J. Phys. Chem. C 114 (2010) 9173–9177.
[34] C.A. Martínez-Huitle, E. Brillas, Appl. Catal. B: Environ. 87 (2009) 105–145.
[35] K.P. Sharma, S. Sharma, Chemosphere 69 (2007) 48–54.
[36] S.M.A.G. Ulson de Souza, E. Forgiarini, A.A. Ulson de Souza, J. Hazard. Mater. 147 (2007) 1073–1078.
[37] C.A. Grimes, J. Mater. Chem. 17 (2007) 1451–1457.
[38] G.K. Mor, O.K. Varghese, M. Paulose, K. Shankar, C.A. Grimes, Sol. Energy Mater. Sol. C 90 (2006) 2011–2075.
[39] I. Paramasivam, H. Jha, N. Liu, P. Schmuki, Small 8 (2012) 3073–3103.
[40] A. Ghicovand, P. Schmuki, Chem. Commun. (2009) 2791–2808.
[41] E. Brillas, M.A. Baños, S. Camps, C. Arias, P.L. Cabot, J.A. Garrido, R.M. Rodríguez, New J. Chem. 28 (2004) 314–322.
[42] R.F.P. Nogueira, M.C. Oliveira, W.C. Paterlini, Talanta 66 (2005) 86–91.
[43] R. Andreozzi, V. Caprio, R. Marotta, D. Vogna, Water Res. 37 (2003) 993–1004.
[44] E.S. Elmolla, M. Chaudhuri, Desalination 252 (2010) 46–52.
[45] M. Harir, A. Gaspar, B. Kanawati, A. Fekete, M. Frommberger, D. Martens, A. Kettrup, M. El Azzouzi, Ph. Schmitt-Kopplin, Appl. Catal. B: Environ. 84 (2008) 524–532.
[46] S. Yang, Y. Liu, C. Sun, Appl. Catal. A: Gen. 301 (2006) 284–291.
[47] O.K. Varghese, C.A. Grimes, J. Nanosci. Nanotechnol. 3 (2003) 277–293.
[48] Y. Zhang, X. Xiong, Y. Han, X. Zhang, F. Shen, S. Deng, H. Xiao, X. Yang, G. Yang, H. Peng, Chemosphere 88 (2012) 145–154.
[49] H. Selcuk, M. Bekbolet, Chemosphere 73 (2008) 854–858.
[50] Y. Murakami, I. Ohta, T. Hirakawa, Y. Nosaka, Chem. Phys. Lett. 493 (2010) 292–295.
[51] P.A. Carneiro, M.E. Osugi, J.J. Sene, M.A. Anderson, M.V.B. Zanoni, Electrochim. Acta 49 (2004) 3807–3820.